TD-DFTB Study of Optical Properties of Silver Nanoparticle Homodimers and Heterodimers

Zhen Liu,[a] Fahri Alkan,[a,b] Christine M. Aikens[a,*]

[a]Department of Chemistry, Kansas State University, Manhattan, KS 66506, USA

[b]Department of Material Science & Nanotechnology Engineering, Abdullah Gül University, Kayseri 38080, Turkey

[*]cmaikens@ksu.edu, 1-785-532-0954, fax: 1-785-532-6666

Abstract

The absorption spectra for face-centered cubic nanoparticle dimers at various interparticle distances are investigated using time-dependent density functional tight binding (TD-DFTB). Both homodimers and heterodimers are investigated in this work. By studying nanoparticles at various interparticle distances and analyzing their vertical excitations, we found that as the interparticle distance decreases, a red shift arises from contributions of the transition dipole moment that are aligned along the z-axis with nondegenerate features; blue shifts occur for peaks that originate from transition dipole moment components in the x and y directions with double degeneracy. When the nanoparticles are similar in size, the features in the absorption spectra become more sensitive to the interparticle distances. The best-fit curves from vertical excitation energy in the form of AR^{-b} for $\Delta E_{redshift}/\Delta E_{blueshift}$ vs. R are determined. In this way, we determined trends for absorption peak shifts and how these depend on interparticle distance.

Introduction

Nanoparticles such as gold and silver have many applications in chemistry, physics, and biology due to their optical properties and their high physical and chemical stability.[1–4] Localized surface plasmon resonances (LSPRs)[5–10] are unique optical characteristics of nanoparticles. The LSPR originates from the collective oscillation of conduction electrons upon excitation with an external electric field. Due to plasmonic coupling, the optical properties of nanoparticles are highly affected by their neighboring particles.[11–16]

A nanoparticle dimer is the simplest system to study nanoparticle interactions. Dimers can provide a model for the systematic study of nanoparticle plasmonic interactions and can pave the way for further understanding of hybridized plasmons[11,17,18] in more complex systems. When the surface plasmons are excited, a large electromagnetic field enhancement can occur in a nanoparticle junction. Studying nanoparticles not only provides physical insights about nanoparticle interaction, but also provides more understanding regarding the resulting electromagnetic field enhancements.[16]

Many previous theoretical studies have employed density functional theory (DFT) and time-dependent density functional theory (TD-DFT)[15,19–28] for describing quantum mechanical effects on the optical properties of large systems.[29–31] Density functional tight binding (DFTB)[32,33] and its time-dependent formalism (TD-DFTB)[34,35] are great potential candidates to improve the computational efficiency of these methods with a small decrease in accuracy. Sanchez and co-workers have used TD-DFTB to investigate the relaxation dynamics of LSPRs in nanoclusters.[36–38] Wong and co-workers used real-time TD-DFTB to study the electron dynamics of a plasmonic antenna and showed the capabilities of TD-DFTB for the calculation of plasmonicity.[39–41] In 2018, Alkan et al. used the TD-DFTB formalism to study the optical properties and electronic structures

of silver nanorods and nanorod dimers.[13] Their results shows a good agreement between TD-DFTB and TD-DFT in that the spectral shapes, energies, and intensity trends from the TD-DFT calculations can be reproduced by TD-DFTB.

Due to the high computational efficiency of DFTB and TD-DFTB, these methods can be used on large systems. Moreover, because DFTB and TD-DFTB allow for explicit treatment of electronic structure, they can more accurately predict absorption spectra compared to classical methods in the cases where quantum mechanical effects become important. Quantum mechanical methods are required to treat effects such as electron tunneling and charge transfer plasmons that are especially evident when the interparticle distance between nanoparticles becomes small. In this study, we employ the TD-DFTB method to examine how the optical properties of homodimers and heterodimers are tuned as the interparticle distance changes. The polarization of the transition dipole moment is an important consideration in dimers. As the distance of the silver nanoparticle dimer decreases, we find that the excitation energy will blue shift when it comes from a dipole transition perpendicular to the dimer interaction axis (i.e. polarized in the x and y directions) and shows up with a doubly degenerate feature. Furthermore, the excitation energy will red shift when it comes from a dipole transition polarized along the dimer interaction axis (z direction) and shows up with no degeneracy. Our study can answer three important questions regarding dimer nanoparticle systems:

(1) Why do new peaks show up upon decreasing the interparticle distance?

(2) When the distance between the nanoparticles in the dimer decreases, why does the highest peak blue shift for some systems and red shift for other systems?

(3) When the distance decreases for one dimer system, what causes the highest peak to blue shift for some distance range, but red shift for another range?

Computational Methods

All density functional tight binding (DFTB) calculations of face-centered cubic (FCC) silver nanoparticles are performed using the Amsterdam Density Functional (ADF) 2016 program.[33–35] Time-dependent density functional tight binding (TD-DFTB)[43–47] calculations are performed using the self-consistent-charge (SCC) formalism and the Hyb-0-2 parameter set.[48,49] The SCC convergence threshold is defined by maximum change between two succeeding SCC cycles. In the calculation, we set the charge convergence tolerance to 1×10^{-9}. The linear-response TD-DFTB method allows for each excited state to be represented with multiple determinants, each of which represents a single orbital-to-orbital transition. Prior to the linear response TD-DFTB calculation, the single orbital transitions with an oscillator strength smaller than 1×10^{-4} are removed, and the rest are coupled into the excited state. The smoothed absorption spectra are convoluted with Gaussian broadening with a full width at half-maximum (FWHM) of 0.05 eV. Because of the high efficiency of TD-DFTB, the largest test case corresponding to the Ag_{164} dimer takes around two hours on one computer node with 15 cores to calculate 4000 excited states for the spectrum.

The geometries of the monomers are created by a FCC coordinate generator using a lattice spacing of 4.0853 Å (from bulk silver) and choosing desired silver FCC spherical radius cutoffs of 4 Å, 7 Å, 8 Å and 8.5 Å. The FCC silver nanoparticles Ag_{14}, Ag_{92}, Ag_{116} and Ag_{164} are generated; their coordinates are provided in the Supporting Information. We construct the dimer structures by using different combinations of monomers at various interparticle distances (6 Å, 7 Å, 8 Å, 9 Å, 10 Å, 12 Å, 15 Å, 17 Å, 20 Å, 25 Å, 30 Å, 40 Å and 50 Å). The distances are measured by considering the distances between the two closest atoms from different nanoparticles in the dimer structure along the z-axis. No geometrical optimizations are performed for these structures.

Four homodimer systems are studied in this work (Figure 1): Ag_{14} dimer, Ag_{92} dimer, Ag_{116} dimer and Ag_{164} dimer. Six heterodimer systems are also examined (Figure 2): Ag_{14} and Ag_{92}, Ag_{14} and Ag_{116}, Ag_{14} and Ag_{164}, Ag_{92} and Ag_{116}, Ag_{92} and Ag_{164}, and Ag_{116} and Ag_{164}.

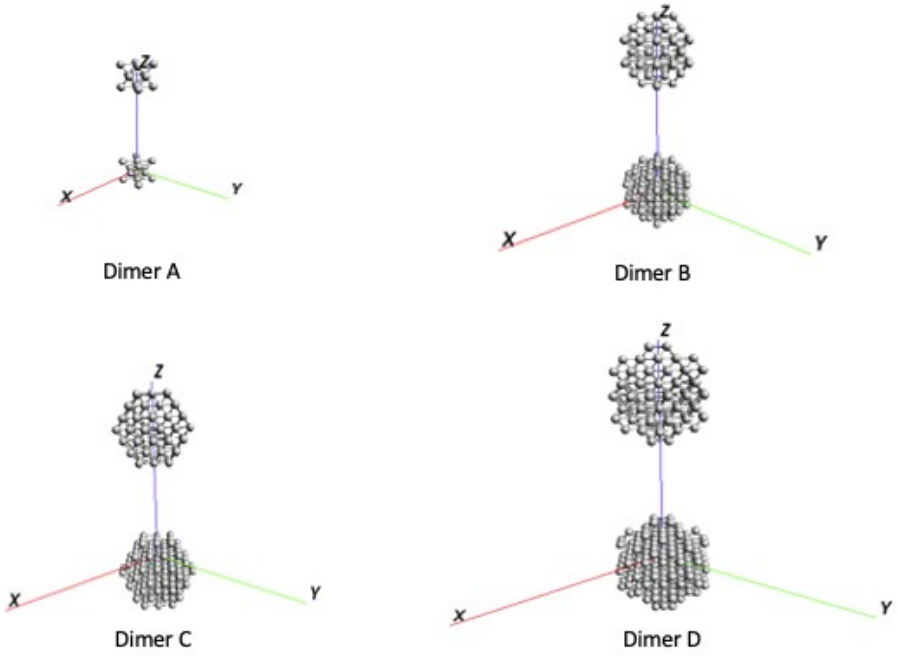

Figure 1. Structures for FCC homodimer nanoparticles

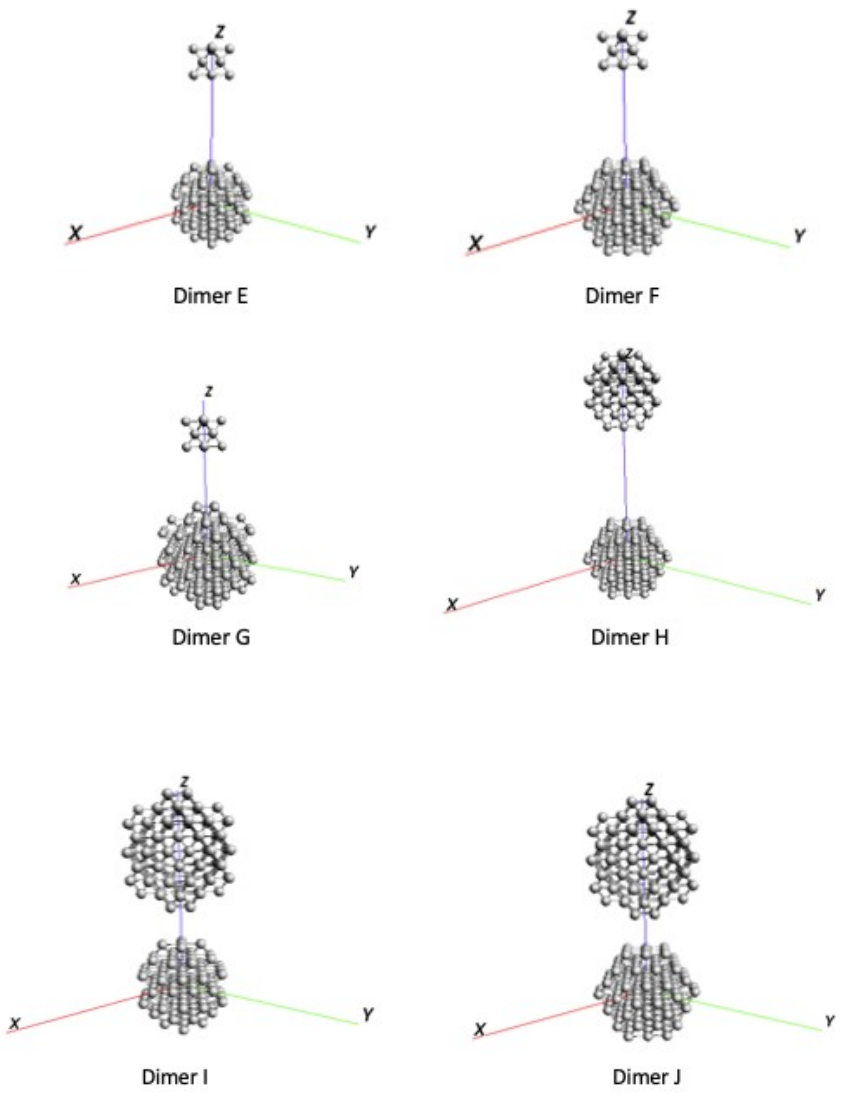

Figure 2. Structures for FCC heterodimer nanoparticles

The interaction between the excited states of two nanoparticles are sometimes treated as a weak perturbation to the Hamiltonian and expressed as a dipole-dipole interaction.[18,50] Then, both $\Delta E_{redshift}$ and $\Delta E_{blueshift}$ would be proportional to $|\mu|^2 R^{-3}$, where μ is the dipole moment of the excited state for the monomer and R is the distance between two dipoles. In this work, the best-fit curves in the form of AR^{-b} for $\Delta E_{redshift}/\Delta E_{blueshift}$ vs. R are determined. In the equation, R is the distance

between the two monomer nanoparticles and A and b are the parameters to be optimized. $\Delta E_{redshift}/\Delta E_{blueshift}$ is the energy difference between the energy of the absorption peak at a given value of R and the energy of absorption at a long distance (50 Å). For optimized A and b, the $\Delta E_{redshift}$ and $\Delta E_{blueshift}$ from the best fit curve agree with the $\Delta E_{redshift}$ and $\Delta E_{blueshift}$ from the TD-DFTB calculation.

In this paper, we present two approaches to analyze the absorption spectra of nanoparticle dimers. In the first approach, we study the highest peak and the overall profile of the absorption spectra and compare with experimental results. The next approach is to analyze individual vertical excitation energies, which are also called "stick spectra". Spectral broadening is included in the first approach by convolving the stick spectra with a Gaussian line shape of a given width. The stick spectra are the source of the simulated absorption spectra. The highest peak in the overall absorption spectrum may be formed from a single excited state with a very high intensity. However, it may also be caused by several close excited states. Thus, it is helpful to employ both approaches when analyzing absorption spectra.

Using the vertical excitation energy information, we can determine the transitions that are responsible for the highest intensity peak and why the highest peak will blue shift at one distance range and red shift over another range. By using the vertical excitation energies, we can analyze a specific excited state, which is critical for studying the absorption peak shifts in nanoparticle dimers. In this paper, we use vertical excited state information to analyze several high intensity peaks. In the vertical excitation energy analysis, we found that the exponential function can be fitted to the energies, whereas it is not feasible to do this for the broadened spectra.

Results and Discussion

Absorption spectra of monomers of FCC-structured silver nanoparticles

Absorption spectra for monomer nanoparticles with different sizes are shown in Figure 3. For $Ag_{14,}$ the strongest peak is located at 3.22 eV (Figure 3a). For $Ag_{92,}$ two strong peaks at 2.87 eV and 2.99 eV are observed (Figure 3b). Numerous low-intensity peaks are also present in this system. Above 3.5 eV, the absorption spectra profile is governed by the high density of states. For $Ag_{116,}$ the highest peak is at 2.87 eV (Figure 3c). Similar to Ag_{92}, the absorption profile above 3.2 eV is determined by the density of states. For $Ag_{164,}$ the absorption spectra profile is determined both by distinct peaks at 2.89 eV and 2.96 eV and the high density of states (Figure 3d). The solid-state features (i.e. that the absorption profile is governed by a high density of states instead of a strong electronic state) become clearer for Ag_{164}.

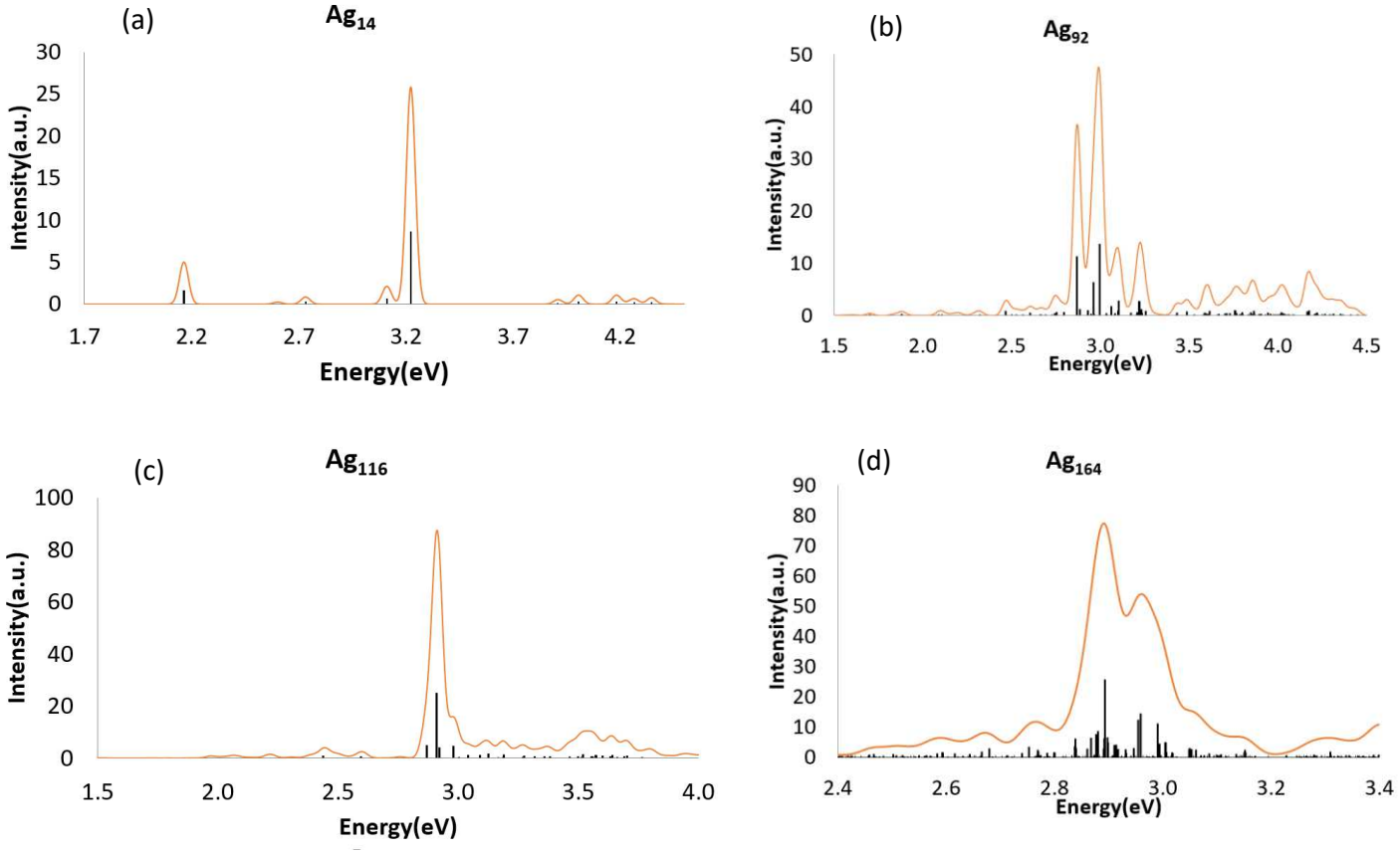

Figure 3. Calculated absorption spectra for FCC silver nanoparticle monomers. (a) Ag_{14}, (b) Ag_{92}, (c) Ag_{116}, (d) Ag_{164}

Absorption spectra of silver nanoparticle homodimers

In this section, we investigate the absorption spectra of homodimers of FCC silver nanoparticles (Ag_{14}, Ag_{92}, Ag_{116}, Ag_{164}) at different interparticle distances (6 Å, 7 Å, 8 Å, 9 Å, 10 Å, 12 Å, 15 Å, 17 Å, 20 Å, 25 Å, 30 Å, 40 Å, 50 Å) (Figure 4).

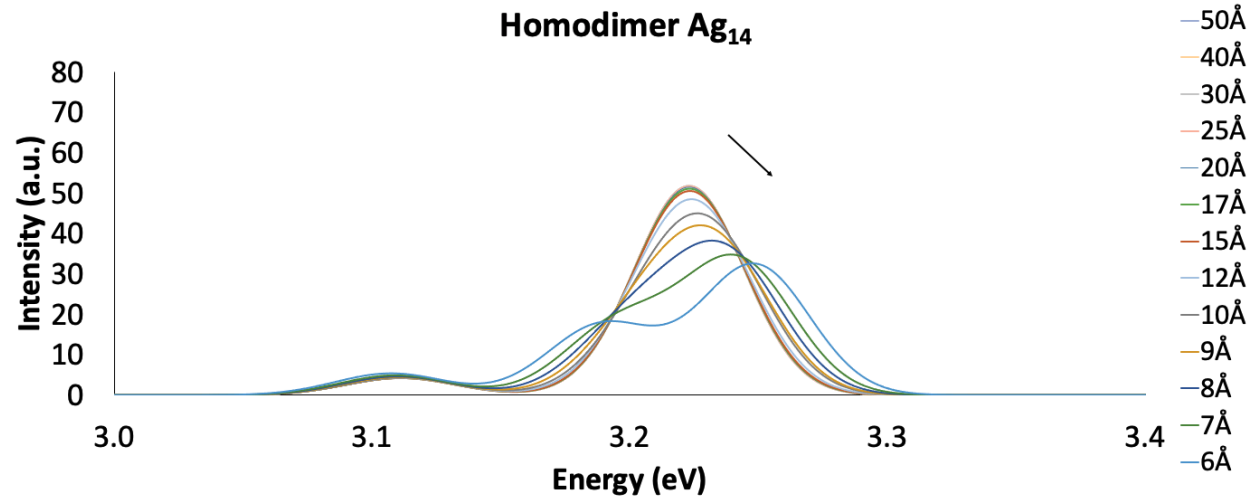
Homodimer Ag_{14}
Intensity (a.u.)
Energy (eV)
50Å
40Å
30Å
25Å
20Å
17Å
15Å
12Å
10Å
9Å
8Å
7Å
6Å

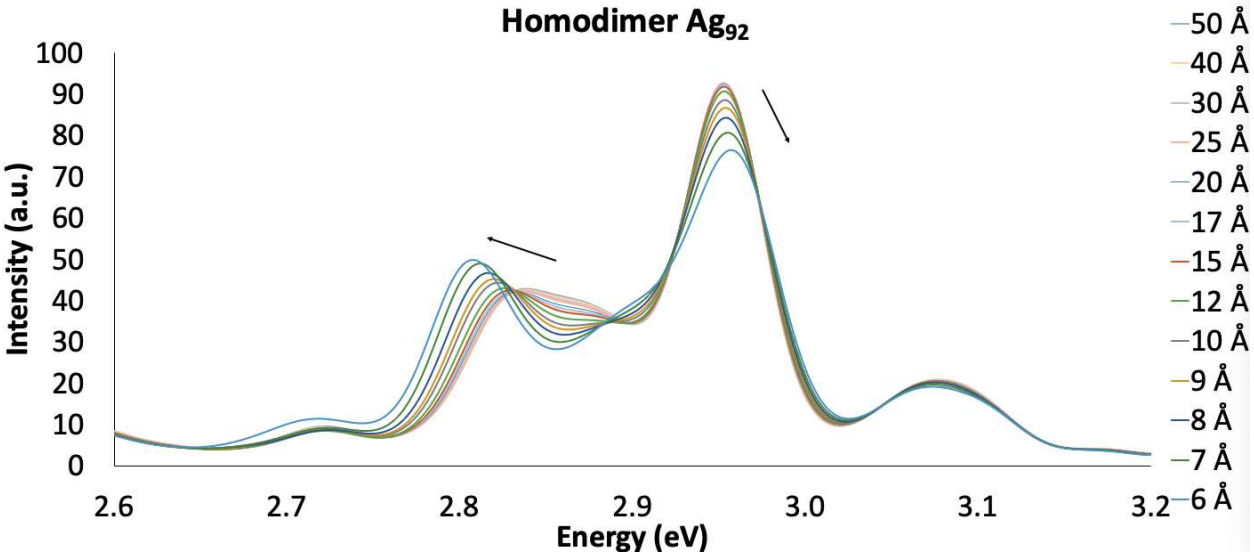
Homodimer Ag_{92}
Intensity (a.u.)
Energy (eV)
50 Å
40 Å
30 Å
25 Å
20 Å
17 Å
15 Å
12 Å
10 Å
9 Å
8 Å
7 Å
6 Å

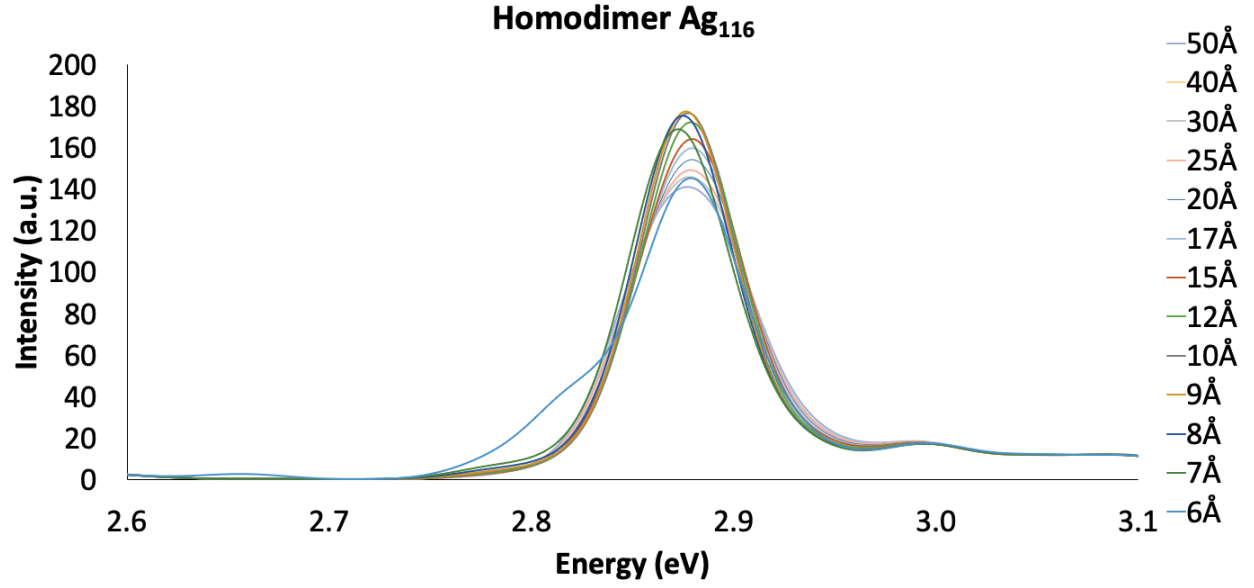
Homodimer Ag_{116}
Intensity (a.u.)
Energy (eV)
50Å
40Å
30Å
25Å
20Å
17Å
15Å
12Å
10Å
9Å
8Å
7Å
6Å

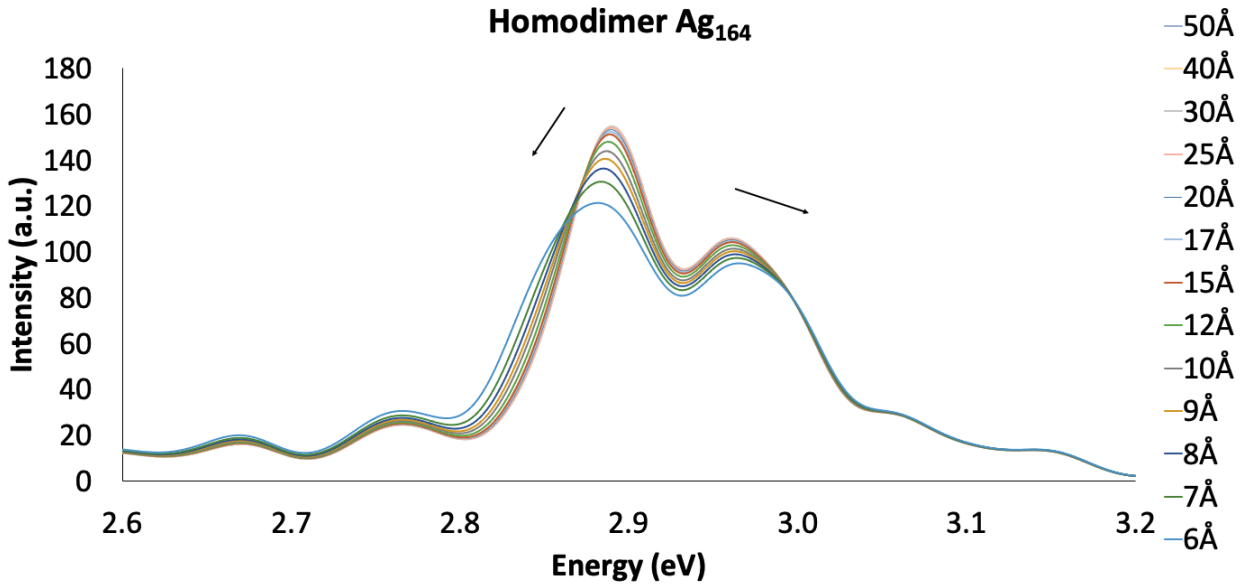

Figure 4. Calculated absorption spectra for FCC silver nanoparticle dimers.

(a) Ag_{14}, (b)Ag_{92}, (c)Ag_{116}, (d)Ag_{164}

For the Ag_{14} dimer (Figure 4a) at an interparticle separation of 50 Å, we found the highest intensity peak at 3.22 eV, which is the same excitation energy as the Ag_{14} monomer. However, the intensity is twice that of the Ag_{14} monomer due to the doubling of the number of electrons in the system. As the interparticle distance decreases from 50 Å to 15 Å, the energies of the highest peaks remain at 3.22 eV. However, from 15 Å to 6 Å, the intensity decreases and the highest peak energy blue shifts from 3.22 eV to 3.24 eV. In addition, a new peak appears at 3.18 eV when the interparticle distance decreases to 6 Å.

For Ag_{92} (Figure 4b), similar characteristics to the Ag_{14} dimer are found. At large interparticle distance (i.e. from 50 Å to 15 Å), the highest intensity peaks all occur at 2.99 eV, similar to the monomer nanoparticle. For this dimer system, the highest peak (at 2.99 eV) blue shifts as the interparticle distance decreases from 15 Å to 6 Å. The second highest peak red shifts from 2.82 eV to 2.81 eV.

For Ag_{116} (Figure 4c) at large interparticle distances, the absorption peaks occur at 2.87 eV, which is the same as the absorption peak of monomer. From 50 Å to 12 Å, the highest absorption peak blue shifts from 2.87 eV to 2.89 eV. From 12 Å to 6 Å, the peak red shifts from 2.89 eV to 2.87 eV. To understand these shifts, it is not sufficient just to analyze the highest peak from the absorption spectrum because the highest peak blue shifts at longer range and red shift at shorter range. However, these shifts can be explained by analyzing the origin of each excitation, via the study of the specific excited states that comprise each strong peak.

For Ag_{164} (Figure 4d), we found that the highest peak red shifts and the second highest peak blue shifts as the distance decreases, which is exactly opposite to the trends for Ag_{92}.

With the discussion above, three specific questions arise: (1) Why does a new peak show up at short distance for the Ag_{14} dimer, or why does the peak split? (2) Why for the Ag_{116} dimer,

does the highest absorption peak blue shift at longer range and red shift at shorter range? (3) Why does the Ag_{164} dimer display opposite trends compared to Ag_{92} with decreasing interparticle distance? All of these questions can be answered by studying the vertical excited states, which correspond to the transitions between different electronic states.

The Ag_{116} dimer is analyzed by studying the excited states that comprise its absorption spectra. In Figures 5-8, the best-fit curve is expressed in the more general form of AR^{-b}, for the calculated $\Delta E_{redshift}$ and $\Delta E_{blueshift}$ at the TD-DFTB level of theory for this system. A similar detailed study of the vertical excitations of Ag_{14}, Ag_{92} and Ag_{164} homodimers can be found in the Supporting Information (Figures S1-S8). The best-fit curve for vertical excitation energies do not follow an AR^{-3} relationship, which is expected because the dipole-dipole interaction does not hold at short distance, due in part to the interaction and mixing of higher multipolar oscillations of nanoparticle dimers.[51,52] The *b* value observed in our work is less than 2, which was the value observed in the "plasmon ruler" work of Jain and El-Sayed.[53,54]

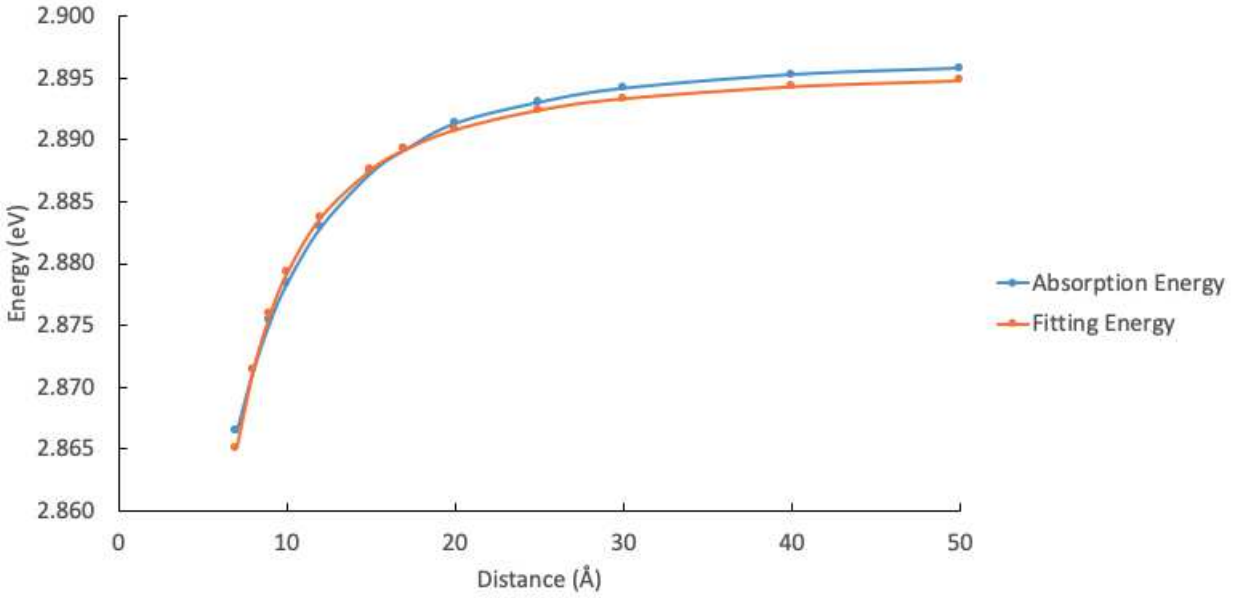

Figure 5. Distance dependence of the absorption energy from the highest intensity excitation of the Ag_{116} dimer and the predicted distance dependence of this absorption energy in the form of $E=AR^{-b}$, where the best-fit curve corresponds to A=-0.8968, b=1.7331

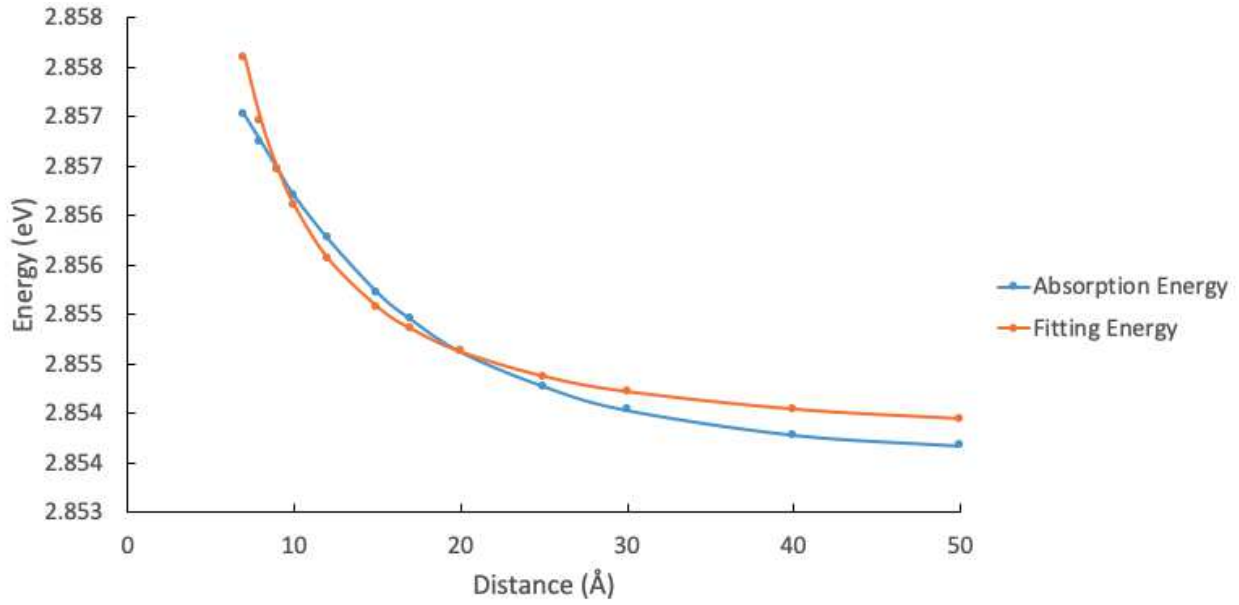

Figure 6. Distance dependence of the absorption energy from the second highest intensity excitation of the Ag_{116} dimer and the predicted distance dependence of this absorption energy in the form of $E = AR^{-b}$, with A=0.0545, b=1.3521

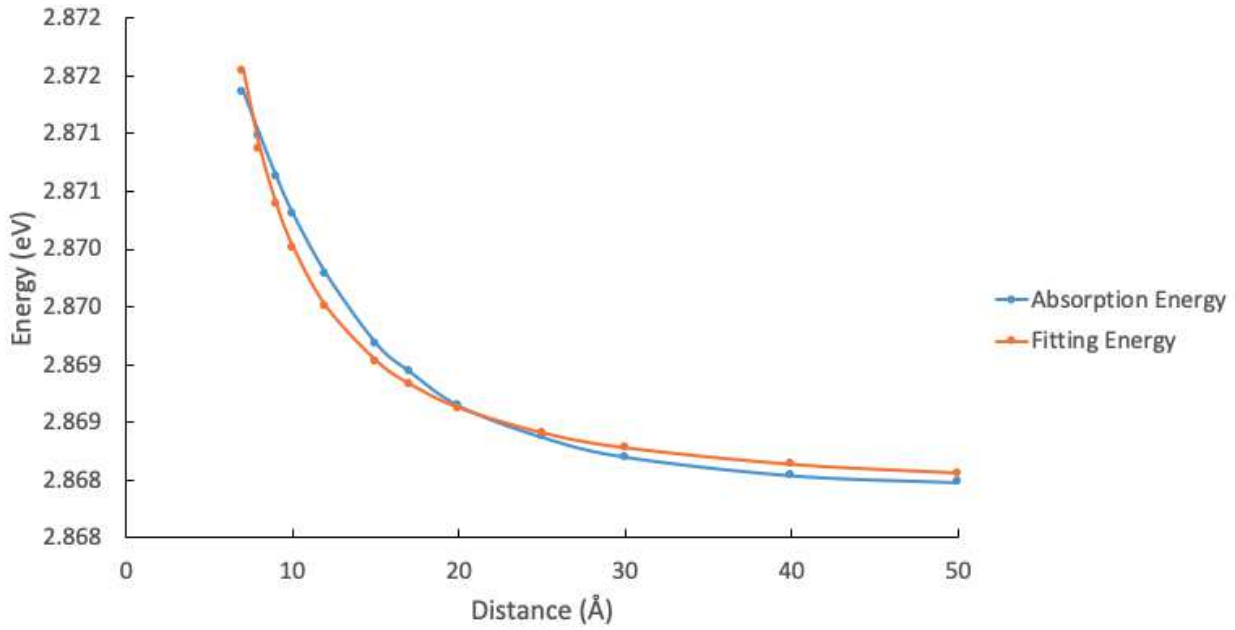

Figure 7. Distance dependence of the absorption energy from the third highest intensity excitation of the Ag_{116} dimer and the predicted distance dependence of this absorption energy in the form of $E = AR^{-b}$, with A=0.0696, b=1.5119

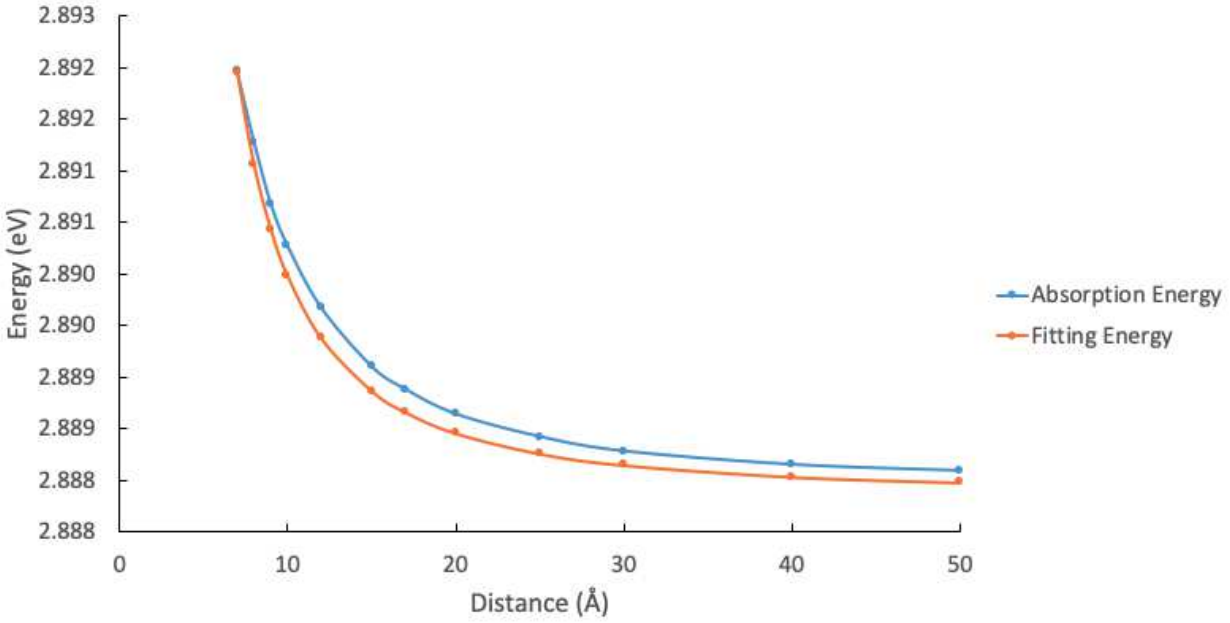

Figure 8. Distance dependence of absorption energy from the fourth highest energy excitation of the Ag_{116} dimer and the predicted distance dependence of this absorption energy in the form of $E = AR^{-b}$, with A=0.1500, b=1.8516

For the Ag_{116} dimer, the vertical excitation energies are shown in Figures 5-8 with detailed data in Tables S1-S4. As shown in Figure 5 and Table S1, as the distance decreases from 50 Å to 6 Å, the highest intensity peak red shifts from 2.90 eV to 2.87 eV. The overall trend of the shifts agrees with distance dependence function AR^{-b} that would be expected from a classical dipole-dipole interaction. Figure 6 and Table S2 show the distance-dependent shift in the second highest intensity peak of the Ag_{116} dimer, which is doubly degenerate. The trend of the second highest peak agrees with a distance dependence function AR^{-b}; however, it has positive sign of A which is the opposite compared to the highest intensity peak, which means that the peak blue shifts as the distance decreases. Figure 7 and Table S3 show a similar trend to the second highest peak with a doubly degenerate state that also fits the distance dependence function; similarly, the peak blue shifts as the interparticle distance decreases. As shown in Figure 8 and Table S4, the fourth highest intensity peak, which is also doubly degenerate, shares similar trends as the second and third highest intensity states.

By analyzing the direction of the transition dipole moment, we found that the highest peak arises from a transition dipole moment in the z direction in agreement with the nondegenerate feature we found in the excitation energy. In contrast, the second, third and fourth highest peaks come from transition dipole moments in the x and y directions, which agree with the doubly degenerate features in the excitation energy. From the plasmon hybridization model,[11,17,18] the interaction of transition dipoles that are oriented along the interdimer axis (in the z direction) lead to a bright state that red-shifts with decreasing interparticle distance (Figure S2), whereas the interaction of transition dipole moments that are perpendicular to the interdimer axis (i.e. in the x and y directions) leads to a bright state that blue-shifts with decreasing distance (Figure S3).

For the three other homodimer systems, the relation between absorption peak shifting and the direction of the transition dipole moment involved is the same as described for Ag_{116} (Figures S4-S25). All transition dipole moments in the z direction are nondegenerate; for these states, as the distance between nanoparticles decrease, the absorption energy red shifts. Double degeneracies are observed for all transition dipole moments in the x and y directions; with decreasing interparticle distance, the absorption energies for these features blue shift.

All of the vertical excitation energies polarized along the z-axis decrease in energy as the distance decreases (corresponding to a negative A value) and all of the vertical excitation energies polarized in the x-y plane increase as the interparticle distance decreases (with a positive A value). When the highest peak is dominated by dipole-dipole interaction polarized along the z-axis, the highest peak in the absorption spectra red shifts as the nanoparticles in the dimer become closer. However, when the highest peak is dominated by dipole-dipole interaction that are polarized in the x-y plane, the highest peak in the absorption spectra blue shifts as the interparticle distance decreases.

When an overall peak in an absorption spectrum has significant contributions from vertical excited states with different polarization, the highest peak can blue shift over a certain range and red shift at another range. As an example, in the Ag_{116} homodimer, the highest peak blue shifts when the nanoparticle distance decreases from 50 Å to 20 Å, and red shifts from 15 Å to 6 Å (Figure 4c). Moreover, by comparing the intensities of the vertical excitations, we found that the highest intensity excitation at 50 Å arises from a z-polarized excitation with an intensity of 57.55, the second highest intensity feature is doubly degenerate and polarized in the x-y plane with an intensity of 26.39. The peak near 2.89 eV in the broadened absorption spectra of Figure 4c arises primarily from a combination of the states presented in Figures 5-8, which means that as the

interparticle distance decreases from 50 Å to 6 Å, one vertical excitation red shifts (Figure 5) while three vertical excitations blue shift. All of these individual shifts combined yields the overall absorption peak shift for Ag_{116}. In the case of Ag_{116}, the total intensity of contributions polarized in the x-y plane combined is close to that polarized along the z-axis. The reason why it is difficult to see a consistent trend for highest energy peak is because the individual vertical excitation energies are very close in energy. This provides an answer for the second question regarding why Ag_{116} experiences a blue shift at intermediate distances and a red shift at the shortest interparticle distance.

Using data from vertical excitation energies of Ag_{14}, we found the highest energy peak red shifts. The energies with double degeneracies blue shift. The new peak that shows up at short distance corresponds to the energy that red shifts, explaining the reason why the new peaks show up upon decreasing the interparticle distance. As the interparticle distance decreases, the highest absorption peak of Ag_{14} is blue shifted; this arises because the absorption profile is dominated by vertical excitation in the z direction whereas vertical excitations in the x and y direction are relatively weaker. At short interparticle distance, the vertical excitation in x and y directions shift to lower energy and become recognizable from the overall profile.

The opposite trend for Ag_{164} compared to Ag_{92} arises because the highest peak for Ag_{164} is dominated by the dipole-dipole interaction in the z-axis and the highest peak for Ag_{92} is dominated by the dipole-dipole interaction polarized in the x-y plane. For Ag_{92}, the dipole-dipole interaction in the x-y plane increases the energy as the interparticle distance decreases, which yields a blue shift in the absorption profile for this peak. On the contrary, for Ag_{164}, the dipole-dipole interaction polarized along the z-axis decreases the peak energy as the interparticle distance decreases, which leads to a red shift trend in the absorption profile. The peak shifting is related to the polarization

direction of the dipole-dipole interaction. In the case of Ag_{116}, the contributions polarized in the x-y plane combined are close to that polarized along the z-axis so that the overall peak shows a blue shift in a certain distance range and a red shift in another distance range in the absorption profile.

Absorption spectra of heterodimer FCC structure silver nanoparticles

Similar to the homodimers at large interparticle distance, the intensity of the absorption spectra of heterodimers is essentially the sum of the intensities of the two constituent monomer nanoparticles, because of the lack of interaction at large interparticle distance. The absorption spectra for heterodimer nanoparticles comprised of different monomer combinations (Ag_{14}, Ag_{92}, Ag_{116}, Ag_{164}) at different distances are shown in Figure 9. For Ag_{14} interacting with Ag_{92} as well as for Ag_{116} interacting with Ag_{164}, only minor peak shifting in the absorption profile is observed (Figure 9a-c), which we attribute to the relatively small size of Ag_{14} compared to the other three nanoparticles. Due to the comparable size and similar absorption energies of Ag_{92}, Ag_{116} and Ag_{164}, the peak shift and the intensity change at different interparticle distances (Figure 9d-9f) is more obvious compared to heterodimer systems involving Ag_{14}. For Ag_{92} interacting with Ag_{116} and Ag_{164}, the absorption peak shifts are relatively large compared to the case when Ag_{14} interacts with Ag_{116} and Ag_{164}. Only a very small shift in the absorption peak occurs when Ag_{92} interacts with Ag_{14} at different distances (Figure 9a). In contrast, the peak shift is much larger when Ag_{92} interacts with Ag_{116} (Figure 9d) at different interparticle distances. We conclude that size is one of the key features for understanding nanoparticle heterodimer optical properties. When monomers are similar in size, the distance-dependent sensitivity of various features in the overall profile of the absorption spectra also increases; for example, peak shifting is found to be greater when two monomers are similar in size. In systems where the two sizes of nanoparticles are relatively distinct, the distance dependent shifts observed in the absorption spectra are relatively weak. Considering the difference in the dominant excitation energy of Ag_{14} and the other nanoparticles, the excitation energy itself is another potential key factor that affects peak shifting in the absorption spectra.

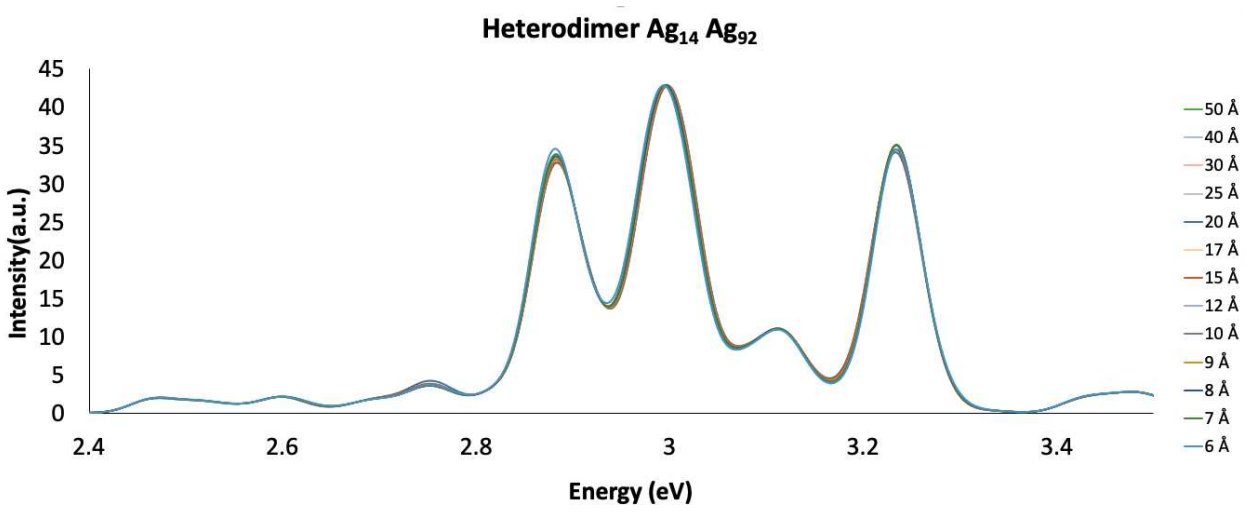
Heterodimer Ag_{14} Ag_{92}
Intensity(a.u.)
Energy (eV)
50 Å
40 Å
30 Å
25 Å
20 Å
17 Å
15 Å
12 Å
10 Å
9 Å
8 Å
7 Å
6 Å

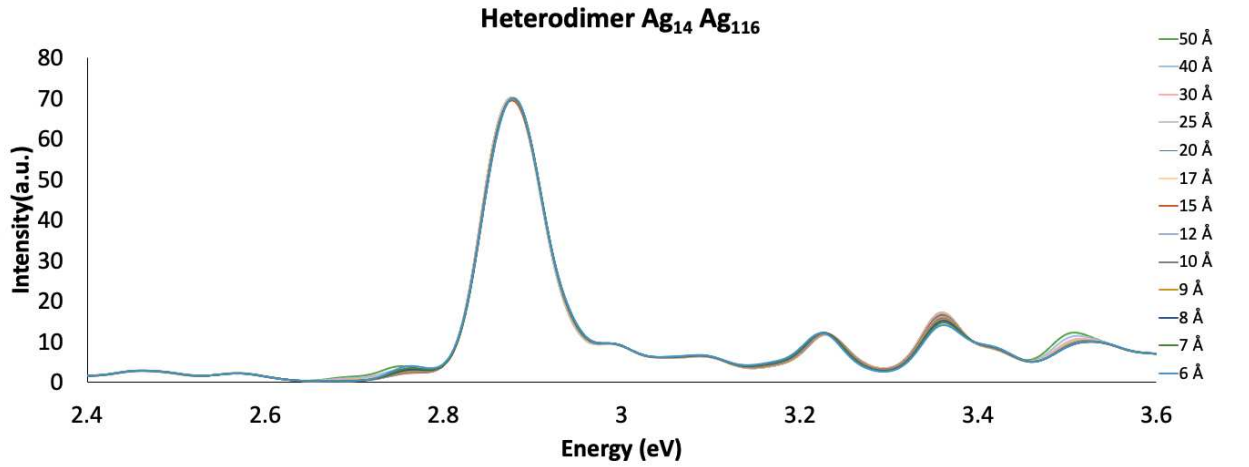
Heterodimer Ag_{14} Ag_{116}
Intensity(a.u.)
Energy (eV)
50 Å
40 Å
30 Å
25 Å
20 Å
17 Å
15 Å
12 Å
10 Å
9 Å
8 Å
7 Å
6 Å

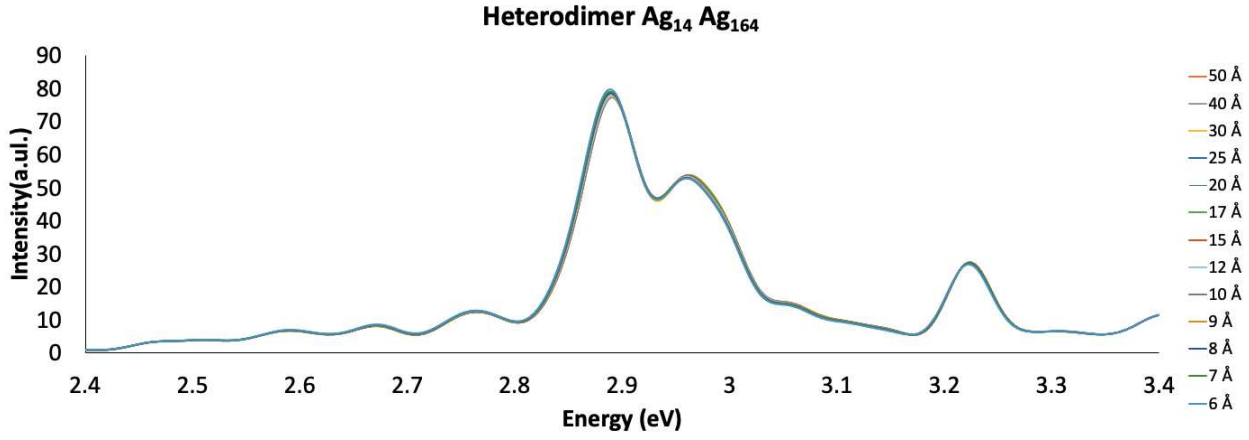
Heterodimer Ag_{14} Ag_{164}
Intensity(a.ul.)
Energy (eV)
50 Å
40 Å
30 Å
25 Å
20 Å
17 Å
15 Å
12 Å
10 Å
9 Å
8 Å
7 Å
6 Å

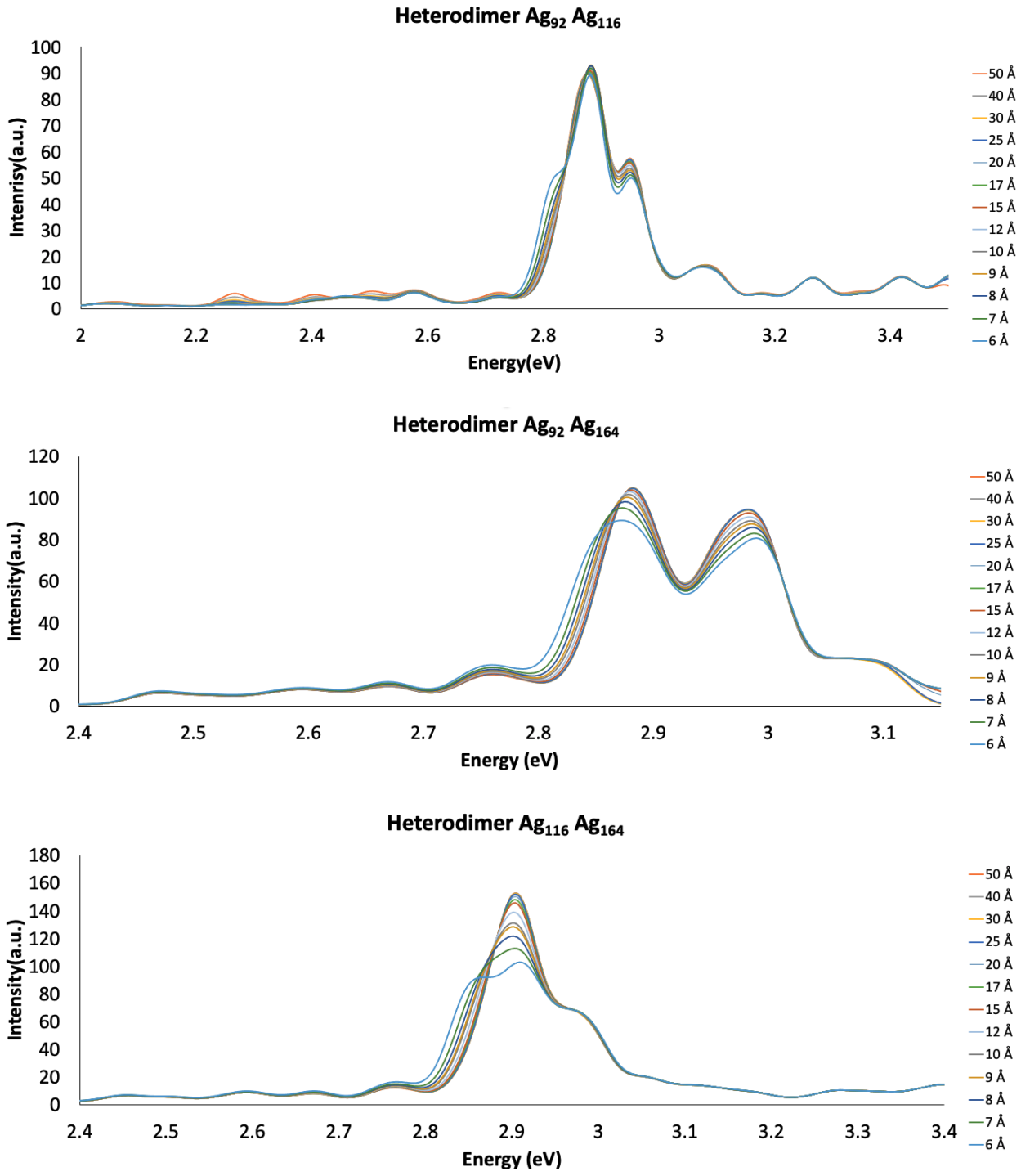

Figure 9. Calculated absorption spectra for FCC silver nanoparticle heterodimers.

(a) Ag_{14} and Ag_{92}, (b) Ag_{14} and Ag_{116}, (c) Ag_{14} and Ag_{164}, (d) Ag_{92} and Ag_{116}, (e) Ag_{92} and Ag_{164}, (f) Ag_{116} and Ag_{164}

For a heterodimer composed of Ag_{116} and Ag_{164}, only one absorption peak is observed at large interparticle distance. When the distance between monomers decreases, the highest peak red shifts and then blue shifts. From Figures S22-S24, we can find the highest peak from absorption profile come from different polarization in similar energy ranges (2.89 eV, 2.91 eV and 2.85 eV). As the distance between nanoparticles get closer, the red shift trend competes with the blue shift. Thus, at large interparticle distances, the dipole-dipole interaction in the z direction is dominant, which appears as the red shift of the highest peak. At shorter distances, the trend is dominated by the dipole-dipole interaction between excitations polarized in the x-y plane; the two different interactions lead to peaks that begin to separate from each other. Starting from interparticle distances of 8 Å and shorter, during the red shifting process the second highest peak becomes distinct from the peak with the highest oscillator strength.

By analyzing the vertical excitation energies, we found that the origin of the absorption at large interparticle distances arises from a combination of the interaction of dipole moments polarized in the z direction and polarized in the x-y plane. As the distance decreases, the interaction of the dipole moment in the z direction is smaller and the interaction of the dipole moment polarized in the x-y plane increases, which corresponds to the red shifts and blue shifts of the peak.

Conclusion

In conclusion, we have investigated the optical properties of monomers and dimers of face centered cubic (FCC) Ag nanoparticles. By theoretically studying the absorption spectra, we can find the origin of the red shifts and blue shifts of absorption peaks. Due to the three-dimensional complexity of isotropic nanoparticles compared to one-dimensional nanowires and nanorods, the transition dipole moments that arise in the FCC dimer system are more complex.

For homodimer nanoparticles with two strong peaks (e.g. homodimer Ag_{92} and homodimer Ag_{164}), one blue shift is observed with the distance decrease from 50 Å to 6 Å, while the other peak red shifts as the dimer get closer. For homodimer nanoparticles with one peak (e.g. homodimer Ag_{14}), the highest peak blue shifts as the distance decreases because the dipole-dipole interaction is polarized in the x-y plane. For Ag_{116}, the dipole-dipole interaction from both z direction and x-y plane are similar in energy so that the highest peak blue shifts 50 Å to 20 Å and the highest peak red shifts from 15 Å to 7 Å. As the interparticle distance decreases, the red shift of the highest peak comes from contributions to the transition dipole moment with components along the z-axis. In contrast, the peak blue shift as interparticle distance decreases mostly comes from the contributions of the transition dipole moment in the x and y directions and shows up with a doubly degenerate feature. This provides a physically intuitive analysis for understanding why the highest peak blue shifts and red shifts at certain distance ranges. The calculated transition energy between different states from DFT methods can be reasonably well fit by a function of the form of AR^{-b} by the classical dipole-dipole interaction analysis.

We also found the size dependence of absorption spectra for heterodimer systems and analyzed them quantitatively. When the difference in the size of the two nanoparticles is large, the spectra are only weakly sensitive to the interparticle distance. However, when the size of two

nanoparticles in a heterodimer system is similar, the distance-dependent features become more sensitive.

In conclusion, TD-DFTB is an efficient method to study large plasmonic systems that contain quantum mechanical characteristics. By studying the vertical excitation energies, we can discover more profound physical meaning than by comparing broadened absorption spectra.

Supplementary Material

See Supplementary Material for tables and figures of interparticle distance vs. peak energy for silver nanoparticle dimers, calculated absorption spectra for silver nanoparticle dimers at 50 Å, plasmon interaction diagrams, and coordinates of FCC silver nanoparticle monomers.

Acknowledgement

This material is based on work supported by the Air Force Office of Scientific Research under Grant FA9550-15-0114. The computing for this project was performed on the Beocat Research Cluster at Kansas State University, which is funded in part by NSF Grants CHE-1726332, CNS-1006860, EPS-1006860, and EPS-0919443.

Data Availability Statement

The data that support the findings of this study are available from the corresponding author upon reasonable request.

References

(1) Huang, X.; El-Sayed, I. H.; Qian, W.; El-Sayed, M. A. Cancer Cell Imaging and Photothermal Therapy in the Near-Infrared Region by Using Gold Nanorods. *J. Am. Chem. Soc.* **2006**, *128* (6), 2115–2120. https://doi.org/10.1021/ja057254a.

(2) Cognet, L.; Tardin, C.; Boyer, D.; Choquet, D.; Tamarat, P.; Lounis, B. Single Metallic Nanoparticle Imaging for Protein Detection in Cells. *Proc. Natl. Acad. Sci.* **2003**, *100* (20), 11350–11355. https://doi.org/10.1073/pnas.1534635100.

(3) Skirtach, A. G.; Dejugnat, C.; Braun, D.; Susha, A. S.; Rogach, A. L.; Parak, W. J.; Möhwald, H.; Sukhorukov, G. B. The Role of Metal Nanoparticles in Remote Release of Encapsulated Materials. *Nano Lett.* **2005**, *5* (7), 1371–1377. https://doi.org/10.1021/nl050693n.

(4) Nie, S. Probing Single Molecules and Single Nanoparticles by Surface-Enhanced Raman Scattering. *Science* **1997**, *275* (5303), 1102–1106. https://doi.org/10.1126/science.275.5303.1102.

(5) Yu; Chang, S.-S.; Lee, C.-L.; Wang, C. R. C. Gold Nanorods: Electrochemical Synthesis and Optical Properties. *J. Phys. Chem. B* **1997**, *101* (34), 6661–6664. https://doi.org/10.1021/jp971656q.

(6) Link, S.; El-Sayed, M. A. Spectral Properties and Relaxation Dynamics of Surface Plasmon Electronic Oscillations in Gold and Silver Nanodots and Nanorods. *J. Phys. Chem. B* **1999**, *103* (40), 8410–8426. https://doi.org/10.1021/jp9917648.

(7) Burda, C.; Chen, X.; Narayanan, R.; El-Sayed, M. A. Chemistry and Properties of Nanocrystals of Different Shapes. *Chem. Rev.* **2005**, *105* (4), 1025–1102. https://doi.org/10.1021/cr030063a.

(8) Eustis, S.; El-Sayed, M. A. Why Gold Nanoparticles Are More Precious than Pretty Gold: Noble Metal Surface Plasmon Resonance and Its Enhancement of the Radiative and Nonradiative Properties of Nanocrystals of Different Shapes. *Chem Soc Rev* **2006**, *35* (3), 209–217. https://doi.org/10.1039/B514191E.

(9) Link, S.; Mohamed, M. B.; El-Sayed, M. A. Simulation of the Optical Absorption Spectra of Gold Nanorods as a Function of Their Aspect Ratio and the Effect of the Medium Dielectric Constant. *J. Phys. Chem. B* **1999**, *103* (16), 3073–3077. https://doi.org/10.1021/jp990183f.

(10) Guidez, E. B.; Aikens, C. M. Quantum Mechanical Origin of the Plasmon: From Molecular Systems to Nanoparticles. *Nanoscale* **2014**, *6* (20), 11512–11527. https://doi.org/10.1039/C4NR02225D.

(11) Nordlander, P.; Oubre, C.; Prodan, E.; Li, K.; Stockman, M. I. Plasmon Hybridizaton in Nanoparticle Dimers. *Nano Lett* **2004**, *4*, 899.

(12) Aćimović, S. S.; Kreuzer, M. P.; González, M. U.; Quidant, R. Plasmon Near-Field Coupling in Metal Dimers as a Step toward Single-Molecule Sensing. *ACS Nano* **2009**, *3*, 1231.

(13) Alkan, F.; Aikens, C. M. TD-DFT and TD-DFTB Investigation of the Optical Properties and Electronic Structure of Silver Nanorods and Nanorod Dimers. *J. Phys. Chem. C* **2018**, *122* (41), 23639–23650. https://doi.org/10.1021/acs.jpcc.8b05196.

(14) Alkan, F.; Aikens, C. M. Understanding Plasmon Coupling in Nanoparticle Dimers Using Molecular Orbitals and Configuration Interaction. *Phys. Chem. Chem. Phys.* **2019**, *21* (41), 23065–23075. https://doi.org/10.1039/C9CP03890F.

(15) Bae, G. T.; Aikens, C. M. TDDFT and CIS Studies of Optical Properties of Dimers of Silver Tetrahedra. *J Phys Chem A* **2012**, *116*, 8260.

(16) Marinica, D. C.; Kazansky, A. K.; Nordlander, P.; Aizpurua, J.; Borisov, A. G. Quantum Plasmonics: Nonlinear Effects in the Field Enhancement of a Plasmonic Nanoparticle Dimer. *Nano Lett* **2012**, *12*, 1333.

(17) Prodan, E.; Radloff, C.; Halas, N. J.; Nordlander, P. A Hybridization Model for the Plasmon Response of Complex Nanostructures. *Science* **2003**, *302*, 419.

(18) Willingham, B.; Brandl, D. W.; Nordlander, P. Plasmon Hybridization in Nanorod Dimers. *Appl Phys B* **2008**, *93*, 209.

(19) Aikens, C. M.; Li, S. Z.; Schatz, G. C. From Discrete Electronic States to Plasmons: TDDFT Optical Absorption Properties of Agn (n = 10, 20, 35, 56, 84, 120) Tetrahedral Clusters. *J Phys Chem C* **2008**, *112*, 11272.

(20) Johnson, H. E.; Aikens, C. A. Electronic Structure and TDDFT Optical Absorption Spectra of Silver Nanorods. *J Phys Chem A* **2009**, *113*, 4445.

(21) Guidez, E. B.; Aikens, C. M. Diameter Dependence of the Excitation Spectra of Silver and Gold Nanorods. *J Phys Chem C* **2013**, *117*, 12325.

(22) Stener, M.; Nardelli, A.; De Francesco, R.; Fronzoni, G. Optical Excitations of Gold Nanoparticles: A Quantum Chemical Scalar Relativistic Time Dependent Density Functional Study. *J Phys Chem C* **2007**, *111*, 11862.

(23) Durante, N.; Fortunelli, A.; Broyer, M.; Stener, M. Optical Properties of Au Nanoclusters from TD-DFT Calculations. *J Phys Chem C* **2011**, *115*, 6277.

(24) Barcaro, G.; Sernenta, L.; Fortunelli, A.; Stener, M. Optical Properties of Silver Nanoshells from Time-Dependent Density Functional Theory Calculations. *J Phys Chem C* **2014**, *118*, 12450.

(25) Weissker, H. C.; Mottet, C. Optical Properties of Pure and Core-Shell Noble-Metal Nanoclusters from TDDFT: The Influence of the Atomic Structure. *Phys Rev B* **2011**, *84*, 165443.

(26) López-Lozano, X.; Barron, H.; Mottet, C.; Weissker, H.-C. Aspect-Ratio- and Size-Dependent Emergence of the Surface-Plasmon Resonance in Gold Nanorods – an Ab Initio TDDFT Study. *Phys Chem Chem Phys* **2014**, *16*, 1820.

(27) Liao, M. S.; Bonifassi, P.; Leszczynski, J.; Ray, P. C.; Huang, M. J.; Watts, J. D. Structure, Bonding, and Linear Optical Properties of a Series of Silver and Gold Nanorod Clusters: DFT/TDDFT Studies. *J Phys Chem A* **2010**, *114*, 12701.

(28) Iida, K.; Noda, M.; Ishimura, K.; Nobusada, K. First-Principles Computational Visualization of Localized Surface Plasmon Resonance in Gold Nanoclusters. *J Phys Chem A* **2014**, *118*, 11317.

(29) Asadi-Aghbolaghi, N.; Rüger, R.; Jamshidi, Z.; Visscher, L. TD-DFT+TB: An Efficient and Fast Approach for Quantum Plasmonic Excitations. *J. Phys. Chem. C* **2020**, *124* (14), 7946–7955. https://doi.org/10.1021/acs.jpcc.0c00979.

(30) D'Agostino, S.; Rinaldi, R.; Cuniberti, G.; Della Sala, F. Density Functional Tight Binding for Quantum Plasmonics. *J. Phys. Chem. C* **2018**, *122* (34), 19756–19766. https://doi.org/10.1021/acs.jpcc.8b05278.

(31) Douglas-Gallardo, O. A.; Berdakin, M.; Frauenheim, T.; Sánchez, C. G. Plasmon-Induced Hot-Carrier Generation Differences in Gold and Silver Nanoclusters. *Nanoscale* **2019**, *11* (17), 8604–8615. https://doi.org/10.1039/C9NR01352K.

(32) Porezag, D.; Frauenheim, T.; Kohler, T.; Seifert, G.; Kaschner, R. Construction of Tight-Binding-Like Potentials on the Basis of Density-Functional Theory – Application to Carbon. *Phys Rev B* **1995**, *51*, 12947.

(33) Seifert, G.; Porezag, D.; Frauenheim, T. Calculations of Molecules, Clusters, and Solids with a Simplified LCAO-DFT-LDA Scheme. *Int J Quantum Chem* **1996**, *58*, 185.

(34) Niehaus, T. A.; Suhai, S.; Sala, F. D.; Lugli, P.; Elstner, M.; Seifert, G.; Frauenheim, T. Tight-Binding Approach to Time-Dependent Density-Functional Response Theory. *Phys Rev B* **2001**, *63*, 085108.

(35) Frauenheim, T.; Seifert, G.; Elstner, M.; Niehaus, T.; Kohler, C.; Amkreutz, M.; Sternberg, M.; Hajnal, Z.; Di Carlo, A.; Suhai, S. Atomistic Simulations of Complex Materials: Ground-State and Excited-State Properties. *J Phys Condens Matter* **2002**, *14*, 3015.

(36) Douglas-Gallardo, O. A.; Berdakin, M.; Sanchez, C. G. Atomistic Insights into Chemical Interface Damping of Surface Plasmon Excitations in Silver Nanoclusters. *J Phys Chem C* **2016**, *120*, 24389.

(37) Bonafé, F. P.; Aradi, B.; Guan, M. X.; Douglas-Gallardo, O. A.; Lian, C.; Meng, S.; Frauenheim, T.; Sánchez, C. G. Plasmon-Driven Sub-Picosecond Breathing of Metal Nanoparticles. *Nanoscale* **2017**, *9*, 12391.

(38) Douglas-Gallardo, O. A.; Soldano, G. J.; Mariscal, M. M.; Sanchez, C. G. Effects of Oxidation on the Plasmonic Properties of Aluminum Nanoclusters. *Nanoscale* **2017**, *9*, 17471.

(39) Ilawe, N. V.; Oviedo, M. B.; Wong, B. M. Real-Time Quantum Dynamics of Long-Range Electronic Excitation Transfer in Plasmonic Nanoantennas. *J Chem Theory Comput* **2017**, *13*, 3442.

(40) Ilawe, N. V.; Oviedo, M. B.; Wong, B. M. Effect of Quantum Tunneling on the Efficiency of Excitation Energy Transfer in Plasmonic Nanoparticle Chain Waveguides. *J. Mater. Chem. C* **2018**, *6* (22), 5857–5864. https://doi.org/10.1039/C8TC01466C.

(41) Oviedo, M. B.; Wong, B. M. Real-Time Quantum Dynamics Reveals Complex, Many-Body Interactions in Solvated Nanodroplets. *J. Chem. Theory Comput.* **2016**, *12* (4), 1862–1871. https://doi.org/10.1021/acs.jctc.5b01019.

(42) te Velde, G.; Bickelhaupt, F. M.; Baerends, E. J.; Fonseca Guerra, C.; van Gisbergen, S. J. A.; Snijders, J. G.; Ziegler, T. Chemistry with ADF. *J. Comput. Chem.* **2001**, *22* (9), 931–967. https://doi.org/10.1002/jcc.1056.

(43) Van Gisbergen, S. J. A.; Snijders, J. G.; Baerends, E. J. Implementation of Time-Dependent Density Functional Response Equations. *Comput. Phys. Commun.* **1999**, *118* (2), 119–138. https://doi.org/10.1016/S0010-4655(99)00187-3.

(44) Rüger, R.; Van Lenthe, E.; Lu, Y.; Frenzel, J.; Heine, T.; Visscher, L. Efficient Calculation of Electronic Absorption Spectra by Means of Intensity-Selected Time-Dependent Density Functional Tight Binding. *J. Chem. Theory Comput.* **2015**, *11* (1), 157–167. https://doi.org/10.1021/ct500838h.

(45) Ru, R.; Lenthe, E. Van; Lu, Y.; Frenzel, J.; Heine, T.; Visscher, L. Correction: Efficient Calculation of Electronic Absorption Spectra by Means of Intensity-Selected Time-Dependent Density Functional Tight Binding (Journal of Chemical Theory and

Computation (2015) 11:1 (157-167) DOI: 10.1021/Ct500838h). *J. Chem. Theory Comput.* **2017**, *13* (7), 3424–3425. https://doi.org/10.1021/acs.jctc.7b00564.

(46) Elstner, M.; Porezag, D.; Jungnickel, G.; Elsner, J.; Haugk, M.; Frauenheim, Th.; Suhai, S.; Seifert, G. Self-Consistent-Charge Density-Functional Tight-Binding Method for Simulations of Complex Materials Properties. *Phys. Rev. B* **1998**, *58* (11), 7260–7268. https://doi.org/10.1103/PhysRevB.58.7260.

(47) Elstner, M.; Frauenheim, T.; Kaxiras, E.; Seifert, G.; Suhai, S. A Self-Consistent Charge Density-Functional Based Tight-Binding Scheme for Large Biomolecules. *Phys. Status Solidi B Basic Res.* **2000**, *217* (1), 357–376. https://doi.org/10.1002/(SICI)1521-3951(200001)217:1<357::AID-PSSB357>3.0.CO;2-J.

(48) Rüger, R.; van Lenthe, E.; Lu, Y.; Frenzel, J.; Heine, T.; Visscher, L.; Szücs, B.; Hajnal, Z.; Frauenheim, Th.; González, C.; Ortega, J.; Pérez, R.; Flores, F.; Rüger, R.; van Lenthe, E.; Lu, Y.; Frenzel, J.; Heine, T.; Visscher, L. Chalcogen Passivation of GaAs(1 0 0) Surfaces: Theoretical Study. In *Applied Surface Science*; North-Holland, 2003; Vol. 212–213, pp 861–865. https://doi.org/10.1016/S0169-4332(03)00016-3.

(49) Szűcs, B.; Hajnal, Z.; Scholz, R.; Sanna, S.; Frauenheim, T. Theoretical Study of the Adsorption of a PTCDA Monolayer on S-Passivated GaAs(l 0 0). *Appl. Surf. Sci.* **2004**, *234* (1–4), 173–177. https://doi.org/10.1016/J.APSUSC.2004.05.181.

(50) Jain, P. K.; El-Sayed, M. A. Plasmonic Coupling in Noble Metal Nanostructures. *Chem Phys Lett* **2010**, *487*, 153.

(51) Ekardt, W. Collective Multipole Excitations in Small Metal Particles: Critical Angular Momentum Lex for the Existence of Collective Surface Modes. *Phys Rev B* **1985**, *32*, 1961.

(52) Khlebtsov, B. N.; Khlebtsov, N. G. Multipole Plasmons in Metal Nanorods: Scaling Properties and Dependence on Particle Size, Shape, Orientation, and Dielectric Environment. *J Phys Chem C* **2007**, *111*, 11516.

(53) Jain, P. K.; Eustis, S.; El-Sayed, M. A. Plasmon Coupling in Nanorod Assemblies: Optical Absorption, Discrete Dipole Approximation Simulation, and Exciton-Coupling Model. *J Phys Chem B* **2006**, *110*, 18243.

(54) Jain, P. K.; Huang, W.; El-Sayed, M. A. On the Universal Scaling Behavior of the Distance Decay of Plasmon Coupling in Metal Nanoparticle Pairs: A Plasmon Ruler Equation. *Nano Lett* **2007**, *7*, 2080.